PROCEEDINGS OF SCIENCE

Comparison of repetition period of whistler-mode chorus and relativistic electron precipitation based on conjunction events of Arase and CALET

Madoka Arai,[a,*] **Yuto Katoh,**[a] **Ryuho Kataoka,**[b] **Shoji Torii,**[c] **Yosui Akaike,**[c] **Mariko Teramoto,**[d] **Atsushi Kumamoto,**[a] **Fuminori Tsuchiya,**[e] **Yasumasa Kasaba,**[e] **Yoshizumi Miyoshi,**[f] **Yosiya Kasahara,**[g] **Shoya Matsuda,**[g] **Iku Shinohara,**[h] **Kazuhiro Yamamoto,**[f] **Ayako Matsuoka,**[i] **Tomoaki Hori**[f] **and Atsuki Shinbori**[f]

[a] *Tohoku University,*
6-3 Aramaki Aza-Aoba, Aoba-ku, Sendai, Miyagi, 980-8578, Japan
[b] *Okinawa Institute of Science and Technology Graduate University,*
1919-1 Tancha, Onna-son, Kunigami-gun, Okinawa, 904-0495, Japan
[c] *Waseda Research Institute for Scienece and Engineering, Waseda University,*
17 Kikuicho, Shinjuku, Tokyo, 162-0044, Japan
[d] *Kyushu Institute of Technology,*
1-1 Sensui-cho, Tobata-ku, Kitakyushu-shi, Fukuoka, 804-8550, Japan
[e] *Planetary Plasma and Atmospheric Research Center, Tohoku University,*
6-3 Aramaki Aza-Aoba, Aoba-ku, Sendai, Miyagi, 980-8578, Japan
[f] *Institute for Space-Earth Environmental Research, Nagoya University,*
Furo-cho, Chikusa-ku, Nagoya, 464-8601, Japan
[g] *Kanazawa University,*
Kakuma-machi, Kanazawa, Ishikawa, 920-1192, Japan
[h] *School of Science, The University of Tokyo,*
7-3-1 Hongo, Bunkyo-ku, Tokyo, 113-0033, Japan
[i] *Data Analysis Center for Geomagnetism and Space Magnetism Kyoto University,*
Kitashirakawa-Oiwake Cho, Sakyo-ku, Kyoto, 606-8502, Japan

E-mail: arai.madoka.r7@dc.tohoku.ac.jp

[*] Speaker

PoS(ICRC2025)1385

The dynamic evolution of Earth's radiation belts is an important topic of space weather research to mitigate the possible malfunctions of satellites orbiting, especially at GEO. Relativistic electron precipitation (REP) detected at LEO indicates when, where, and how the loss process of radiation belt electrons takes place. REP is detected as the enhancement of downward electron counts in the MeV energy range. Pitch angle scattering by whistler-mode chorus emissions in the magnetosphere is a plausible mechanism responsible for REP. Previous studies revealed that the repetition periods of REP and chorus are statistically similar, but those in the simultaneous observation of REP and chorus have not been analyzed yet.

In this study, we investigated the repetition periods of both REP and chorus based on the conjunction events of the ISS/CALET at LEO and the Arase satellite in the magnetosphere. We defined REP by using the count rates observed with CALET's CHarge Detector (CHD) as the ratio of CHD-X (upper layer) to CHD-Y (lower layer) count rates $\geq$1.2. The threshold energies to detect the precipitating electrons are 1.6 MeV and 3.6 MeV for CHD-X and CHD-Y, respectively. Chorus appears in the spectra with a hierarchical time scale consisting of several hundred milliseconds, corresponding to the repetition of each chorus element, and a few seconds, corresponding to a group of chorus elements. The same hierarchical time scale can be expected for REP. We used CHD count-rate data with a 1-second time cadence to investigate the fluctuations of REP in seconds. Additionally, we used higher time-resolution count-rate data with a time resolution of up to 20 Hz to investigate the fluctuations of REP in hundred milliseconds. Similarly, we analyzed the repetition periods of chorus emissions using Arase satellite data. We use Arase/WFC data, which measures 64 kHz sampled waveforms over limited time intervals, to analyze the fine-scale structure of individual chorus elements and compare them with the repetition period of REP on a millisecond time scale. The present study reveals that the repetition periods of REP occurred in a time scale corresponding to the chorus elements observed in the magnetosphere.

39th International Cosmic Ray Conference (ICRC2025)
15 - 24 July, 2025
Geneva, Switzerland

1. Introduction

Solar activity causes various phenomena that affect our daily lives, collectively called space weather [1]. Relativistic electron precipitation (REP) is one of space weather in which electrons with a kinetic energy greater than one million electron volts (MeV) trapped in the radiation belt are lost into the Earth's atmosphere [2]. It is thought to be a result of the pitch angle scattering of relativistic electrons by plasma waves in the magnetosphere, but the detailed mechanism is not fully understood [3]. Since relativistic electrons cause extra exposure to radiation for astronauts during extravehicular activities and satellite malfunction, it is important to clarify the mechanism of REP events.

Whistler-mode chorus emissions are electromagnetic plasma waves that naturally occur around the equatorial region of the magnetosphere. Chorus appears in the spectra with a hierarchical time scale consisting of several hundred milliseconds, corresponding to the repetition of each chorus element, and a few seconds, corresponding to a group of chorus elements. Chorus causes the pitch angle scattering of electrons in a wide energy range from thousands of electron volts (keV) to MeV. Since the precipitation of keV electrons contributes to auroral emissions, there is a correspondence between chorus wave amplitude and auroral intensity variations [4][5]. The pitch angle scattering of MeV electrons by chorus occurs in high latitude regions, but usually chorus deviates from the magnetic field line during its propagation and does not reach there. A plasma density structure that guides the waves, known as a duct, is considered necessary to cause REP.

In this study, we investigate the role of chorus in REP events observed by the Calorimetric Electron Telescope (CALET) and the Monitor of All-sky X-ray Image (MAXI) on board the International Space Station (ISS) and the Arase and Van Allen Probes satellites. In particular, we focus on identifying the region where REP occurred and the repetition periods of REP and chorus.

2. Method

The CHarge Detector (CHD) of CALET consists of two orthogonal layers of plastic scintillators (CHD-X and CHD-Y) with a detection threshold corresponding to ≥1.6 MeV and ≥3.6 MeV electrons, respectively [1]. We define the REP event by the ratio between the CHD-X and CHD-Y count rates ≥1.2. We use CHD count rate data with a 1-second time cadence to investigate the fluctuations of REP in seconds. We also use count rate data with a time resolution of up to 20 Hz to investigate the subsecond variations of REP. MAXI's Radiation Belt Monitor (RBM) measures the horizontal direction with RBM-H and the zenith direction with RBM-Z in the time resolution of one-second with the threshold for electrons above 300 keV [7]. For the analysis of chorus, we use the data from the waveform capture (WFC) and the onboard frequency analyzer (OFA) of the Plasma Wave Experiment (PWE) of Arase [8], and the Electric and Magnetic Field Instrument Suite and Integrated Science (EMFISIS) of Van Allen Probes (VAP) [9]. The sampling frequency of the waveform used in this study is 64 kHz in Arase and 35 kHz in VAP.To compare the subsecond variations of REP with the occurrence intervals of chorus elements, we apply the algorithm developed by O'Brien et al. [6]. We define a peak as $\frac{N-A_t}{\sqrt{1+A_t}} > x$, where N is the number of counts or chorus intensity, A_t is the running average over t seconds, and x is the threshold. For CALET/CHD higher time-resolution data, we apply $t = 0.5$ and $x = 1$ and define the time interval between detected peaks as the repetition period. The repetition period of chorus elements

is investigated applying $t = 0.5$ and $x = 10$ to the time series of integrated wave magnetic field spectra over 1–10 kHz where chorus dominates with the power spectral density $\geq 10^2$ [pT^2/Hz].

3. Results

Figure 1 shows the REP event on 11 September 2018. When the footprints of VAP-B and Arase approached that of ISS (Figs.1ab), chorus was observed by VAP-B (Figs.1cd) and Arase (Figs.1ef) in the magnetosphere, while MAXI/RBM and CALET/CHD count rates increased in the same time interval, indicating electron precipitation in the energy range from hundreds of keV to MeV at low altitudes (Figs.1gh). The increase of the count rates of RBM-Z occurred continuously from 0748 UT to 0753 UT, whereas the count rates of CHD increased intermittently with different time scales. We find that REP occurred in both localized and wide L-value ranges. We investigated the range of L-value (ΔL) during the three time intervals where REP occurred (shown in red, blue, and magenta in Fig.1i), as summarized in Table 1. We compared ΔL with regions where chorus occurred, as observed by VAP-B. Between 0749 UT to 0755 UT, when the distance between the footprints of ISS and VAP-B was less than 0.2 in the L-value (Fig.2b), the interval of the hundreds of keV electron precipitation corresponded with the appearance of chorus (Figs.1d, 1g, and 2a), while REP occurred in the limited interval (Fig.1h). We calculated the cyclotron resonance condition with chorus observed by VAP-B (Fig.2c). The solid line in Fig.2c indicates the loss cone angle

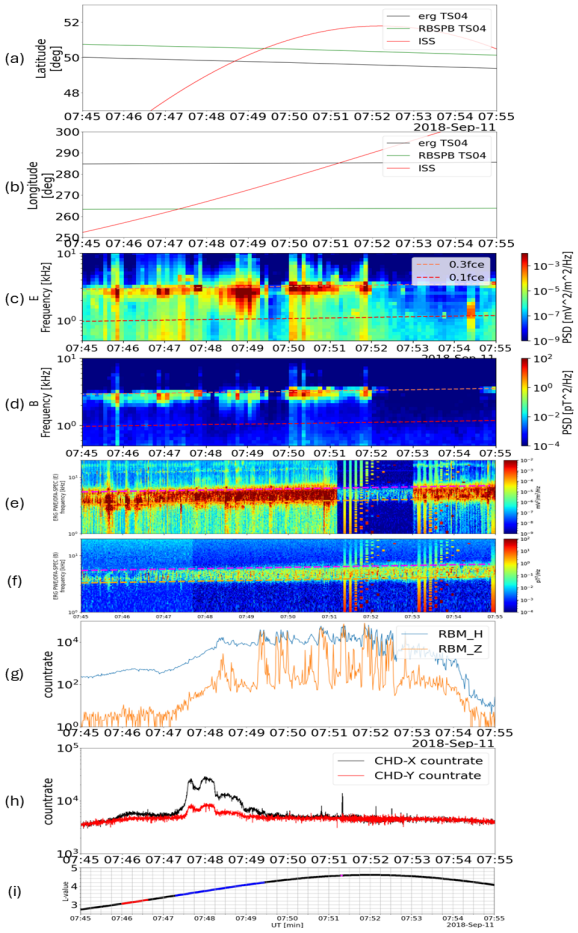

Figure 1: (a) Latitude and (b) longitude of footprints of ISS (red), Arase (black), and VAP-B (green) on 11 Sep 2018. (c) Wave electric and (d) magnetic field spectra measured by VAP-B/EMFISIS; dashed lines show 0.3 times (orange) and 0.1 times (red) the electron cyclotron frequency. (e) Wave electric and (f) magnetic field spectra measured by Arase/PWE; dashed lines show 0.5 times (magenta) and 0.3 times (orange) the electron cyclotron frequency. Count rates detected by (g) MAXI/RBM and (h) CALET/CHD. (i) L-value of ISS. The time intervals of the REP events used to analyze ΔL are shown in red, blue, and magenta.

Table 1: L-value region where REP occurred.

REP duration	L_{start}	L_{end}	ΔL
07:46:00 - 07:46:37	3.06	3.26	0.20
07:47:18 - 07:49:26	3.50	4.20	0.70
07:51:18 - 07:51:19	4.5747	4.5748	0.0001

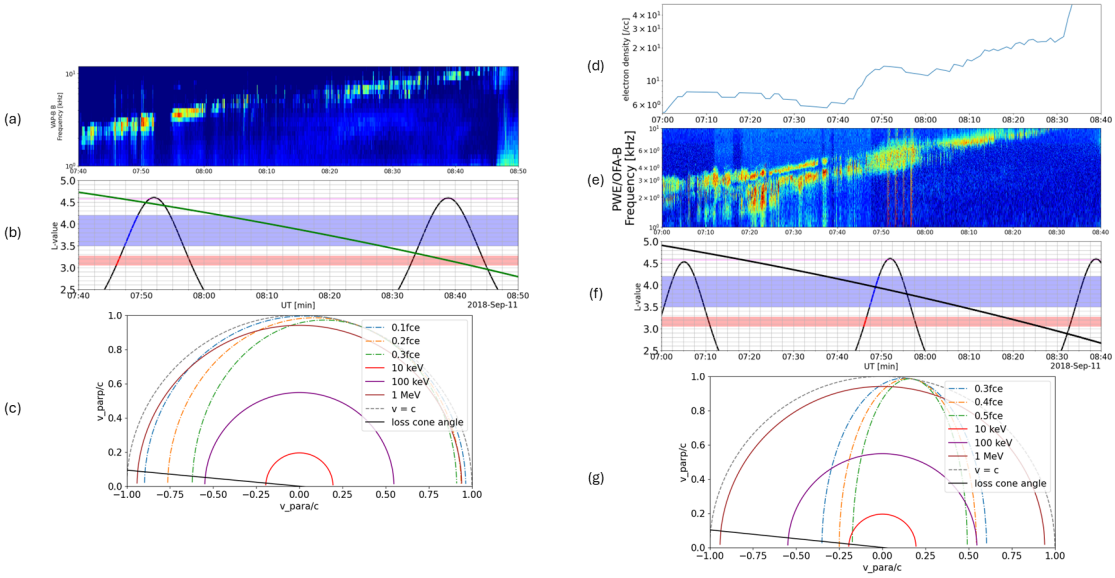

Figure 2: (a) The magnetic field component of spectra data observed by VAP-B/EMFISIS. (b) L-value of ISS (black) and VAP-B (green). The range of L-values given in Table 1 are shown in red, blue, and magenta. (c) The resonance curve was calculated using geomagnetic parameters observed by VAP-B. The dashed lines indicate the frequencies of chorus waves observed by VAP-B, the solid semi-circles represent the constant electron energy curves, and the black solid line shows the loss cone angle at the position where VAP-B observed the chorus waves. (d) The electron density determined based on the Arase/PWE observation. (e) The magnetic field component of spectra observed by Arase/PWE/OFA. (f) L-value of ISS (curved line) and Arase (straight line). (g) The resonance curves calculated using ambient parameters observed by Arase. The dashed lines indicate the frequencies of chorus waves observed by Arase.

$\alpha_{\rm loss}$ = 5.36° at the VAP-B position (L = 4.28, magnetic latitude 10.73°), where electrons having the pitch angle smaller than $\alpha_{\rm loss}$ precipitate into the atmosphere. It was found that chorus in the frequency range $\leq 0.3 f_{ce}$ observed by VAP-B resonate with electrons inside the loss cone in the energy range observed by MAXI/RBM.

We compared ΔL with regions where chorus observed by Arase (Figs.2ef). Arase observed chorus for several minutes around L=4, where REP was detected by ISS. Fig.2g shows the cyclotron resonance condition with chorus observed by Arase. It was found that chorus in the frequency range $\geq 0.3 f_{ce}$ observed by Arase do not resonate with electrons in the energy range greater than 30 keV at the location of the Arase observation. This result indicates that the presence of a duct should be considered to explain the precipitation of high-energy electrons observed by the ISS. We investigated whether the observed chorus could propagate to high latitudes by ray tracing, which is a technique used to simulate the propagation of waves based on the electron density structure in

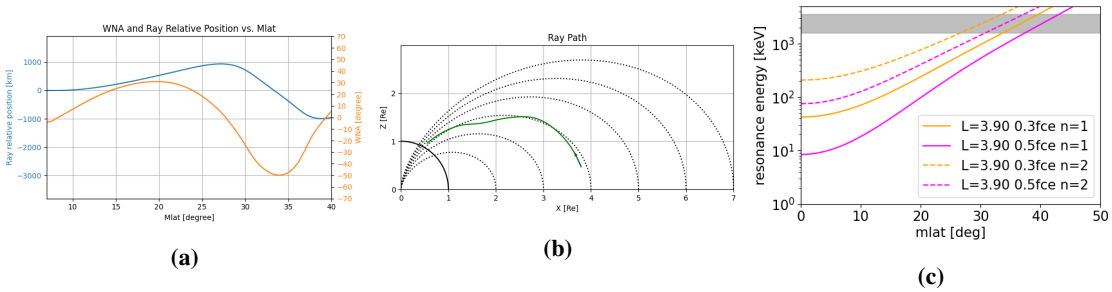

(a) **(b)** **(c)**

Figure 3: (a) Wave normal angle (WNA, orange line) and ray relative position (blue line) as functions of magnetic latitude (Mlat). (b) Ray path of a chorus wave traced in the meridional plane. The green line shows the trajectory of the wave, while the dotted lines represent geomagnetic field lines at different L-shells. The black arc indicates the Earth's surface. (c) Magnetic latitude dependence of the resonant energy for chorus waves propagating along density structures. The solid and dashed lines indicate the resonant energy corresponding to the first (n=1) and second (n=2) order cyclotron resonance conditions, respectively.

the magnetosphere [10][11]. In this study, we performed ray tracing using the parameters observed by Arase under the assumption that the density gradient between 07:45 and 08:00 UT acted as a duct (Figs.2d). We assumed a Gaussian-shaped density enhancement structure (14 cm^{-3} at a peak) with a width of 3812 km (0.6 Earth radius) on a background of 7 cm^{-3}. We trace the ray path of whistler-mode waves of frequency of 0.3 f_{ce} injected from the equator of L=3.9. Figures 3ab indicate that as the wave propagates toward higher latitudes, it is refracted by the plasma density gradient, and the wave normal angle changes accordingly. The results suggest a possibility that the chorus observed by Arase can reach higher latitudes. Fig.3c shows the resonance energy of whistler-mode waves of frequency of 0.3 and 0.5 f_{ce} as a function of magnetic latitude along the field line of L=3.9, where the first (n=1) and second order (n=2) cyclotron resonance conditions are considered. The results suggest that the resonance energy reaches the MeV energy range if chorus propagates the magnetic latitude larger than 25 degree.

Finally, we calculated the repetition period of REP and chorus. Figure 4 shows the distributions of the repetition period of peaks in the CHD count rates and the wave power observed by VAP-B and Arase. We used the data observed between 07:30-08:00 UT, where the waveform data of both VAP-B and Arase are available (Figs.4c, 4d). We also plotted the distribution of peaks in background, where we define background as when the ratio between CHD-X and CHD-Y count rates is <1.2. Figure 4 indicates that the distributions of REP and chorus element both peaked at 0.2-0.4 second repetition period. A comparison between Figures 4a and 4b shows that the number of repetition periods longer than 1 second is nearly the same between CHD-X and CHD-Y, whereas the events showing the repetition periods shorter than 1 second are almost half in the CHD-Y data compared to the CHD-X data.

4. Discussion

We found in Figure 1 that the precipitation of hundreds of keV electrons occurred continuously over a broad region, whereas REP appeared intermittently with different time scales, as summarized in Table 1. Although previous studies reported a close correspondence between chorus and REP, the present study reveals that REP does not always occur in all regions where chorus was present. The

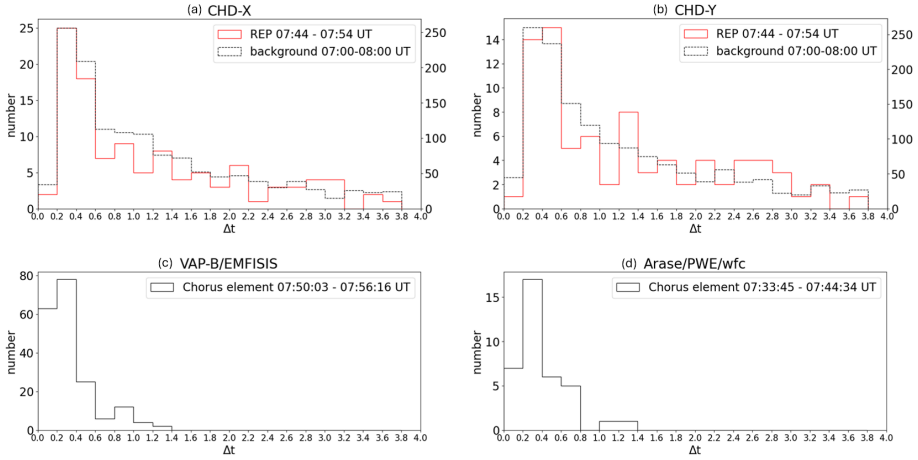

Figure 4: (a) Repetition period of REP observed by CHD-X. The red line and the left vertical axis show repetition periods of REP, while the dotted line and the right vertical axis show that of background. (b) Repetition period of REP observed by CHD-Y. (c) Repetition period of chorus element observed by VAP-B. (d) Repetition period of chorus element observed by Arase.

result suggests that the presence of chorus alone is not sufficient to trigger REP and that additional factors should be involved. Figure 3 implies that chorus may have propagated to higher latitudes due to the ambient plasma density structure, potentially contributing to REP generation.

The new finding of this paper is that of the repetition periods revealed that both REP and chorus element exhibited peak of 0.2-0.4 seconds. The difference between CHD-X and Y indicates the REP with the repetition periods shorter than 1 second occurs relatively less frequently in the higher energy range (>3.6 MeV). Considering that the resonance energy increases as the magnetic latitude increases (Fig.3c), the difference between CHD-X and CHD-Y distributions may indicate the propagation properties of chorus elements along a field line; fewer chorus elements reach higher magnetic latitude. These results support the idea that REP was generated through mechanisms involving the propagation of chorus to higher latitudes. The spatial extent and regional variation of REP occurrence reflect the efficiency and range of such mechanisms, which are likely influenced by local plasma conditions and the surrounding magnetospheric environment.

5. Summary

REP events were identified using a criteria of the CHD-X/Y count rate ratio $\geq$1.2. Chorus were analyzed using waveform data from Arase/PWE and VAP/EMFISIS, and their repetition periods, particularly on subsecond scales, were quantitatively characterized using a peak detection algorithm.

On 11 September 2018, electron precipitation ranging from hundreds of keV to MeV energies was observed at the ISS, while chorus were simultaneously detected by Arase and VAP at nearby L-value. The precipitation of hundreds of keV electrons appeared to be synchronized with the occurrence of chorus observed VAP-B, whereas REP was more localized. Furthermore, ray tracing using parameters from Arase indicated that chorus could propagate to higher latitudes due to the plasma density enhancement, enabling chorus to resonate with MeV electrons. The distribution of the repetition periods of REP and chorus elements showed a common peak at 0.2–0.4 seconds.These

findings support the possibility that REP is triggered by chorus propagated to higher magnetic latitude. Since REP doesn't occur in all regions where chorus is present, the formation of localized plasma environments that facilitate high latitude propagation of chorus may be a key condition for chorus-induced REP.

Acknowledgements

We thank all members of the CALET collaboration for providing the CHD count rate data and supporting this research. The MAXI/RBM data used in this study were provided by RIKEN, JAXA, and the MAXI team, which are available via DARTS at JAXA. The CALET/CHD data (http://darts.isas.jaxa.jp/pub/calet/cal-v1.0/CHD/level1.1/) and MAXI/RBM data (http://darts.isas.jaxa.jp/pub/maxi/rbm/) were provided at DARTS website. Both the data and input files necessary to reproduce the experiments with CALET/CHD higher time-resolution data are available from the authors upon request (torii.shoji@waseda.jp). This study is supported by Grants-in-Aid for Scientific Research (23H05429, 23K25925, and 24H00025) of Japan Society for the Promotion of Science.

Science data of the ERG (Arase) satellite were obtained from the ERG Science Center operated by ISAS/JAXA and ISEE/Nagoya University (https://ergsc.isee.nagoya-u.ac.jp/index.shtml.en, Miyoshi, Hori et al.,2018).

References

[1] Kataoka et al., *Geophysical Research Letters*, **43**, 4119–4125 (2016) [doi:10.1002/2016GL068930].
[2] Kataoka et al., *Journal of Geophysical Research*, **125**, (9) (2020) [doi:10.1029/2020JA027875].
[3] Ueno et al., *Space Weather*, **18**, (7) (2019) [doi:10.1029/2019SW002280].
[4] Ozaki et al., *Geophysical Research Letters*, **45**, (22) (2018) [doi:10.1029/2018GL079812].
[5] Hosokawa et al., *Sci Rep*, **10**, (3380) (2020) [doi:10.1038/s41598-020-59642-8].
[6] O'Brien et al., *Journal of Geophysical Research: Space Physics*, **108**, (A8), (2003) [doi:10.1029/2002JA009784].
[7] Mihara et al., *Handbook of X-ray and Gamma-ray Astrophysics*, 1–25, (2022) [doi:10.1007/978-981-16-4544-0_38-1].
[8] Kasahara et al., *Earth, Planets and Space*, **70**, 86, (2018) [doi:10.1186/s40623-018-0842-4].
[9] Kletzing et al., *Space Science Reviews*, **179**, 127–181, (2013) [doi:10.1007/s11214-013-9993-6].
[10] Kimura et al., *Radio Science*, **1**, (3), 269–284, (1966) [doi:10.1002/rds196613269].
[11] Tachi and Katoh, *Earth, Planets and Space*, **76**, 166, (2024) [doi:10.1186/s40623-024-02109-1].
[12] Kumamoto et al., *Earth, Planets and Space*, **70**, (2018) [doi:10.1186/s40623-018-0854-0].
[13] Matsuda et al., *Earth, Planets and Space*, **70**, (2018) [doi:10.1186/s40623-018-0838-0].
[14] Matsuoka et al., *Earth, Planets and Space*, **70**, 43, (2018) [doi:10.1186/s40623-018-0800-1].
[15] Miyoshi et al., *Earth, Planets and Space*, **70**, (2018) [doi:10.1186/s40623-018-0862-0].
[16] Miyoshi et al., *Earth, Planets and Space*, **70**, (2018) [doi:10.1186/s40623-018-0867-8].